

Temperature dependence of the electric field gradient at Ta impurities in the heavy-rare-earth metals Gd, Dy, Ho, and Er

M. Forker and W. Steinborn

*Institut für Strahlen und Kernphysik der Universität Bonn,
Bonn, Federal Republic of Germany*

(Received 8 February 1979)

The time-differential perturbed-angular-correlation (TDPAC) technique has been used to study the temperature dependences of the electric field gradient (EFG) at ^{181}Ta impurities in the heavy-rare-earth (R) metals Gd, Dy, Ho, and Er. At room temperature the ratio $\alpha \equiv |V_{zz}/(1-\gamma_\infty)V_{zz}^{\text{lat}}|$ of the measured EFG V_{zz} and the calculated ionic EFG $(1-\gamma_\infty)V_{zz}^{\text{lat}}$ decreases linearly with increasing rare-earth atomic number. A linear but much stronger decrease of α has previously been reported for the impurity ^{111}Cd . A simple model is proposed which explains the linear decrease of α and the different slopes for ^{181}Ta and ^{111}Cd in terms of the lanthanide contraction. This model assumes the conduction-electron contribution to the EFG to be mainly determined by the number of electrons in the Wigner-Seitz cell of the impurity. In all rare-earth hosts the EFG decreases with increasing temperature. This decrease, which is slightly stronger for Gd than for Er, is better described by a linear function of temperature than by a $T^{3/2}$ behavior, observed in many other impurity-host systems. The temperature dependence of the EFG is much stronger than expected from the lattice expansion. The difference between the temperature dependence of the measured EFG and of the calculated lattice EFG decreases across the rare-earth series. This can be attributed to a decrease of the amplitudes of the lattice vibrations between Gd and Er.

I. INTRODUCTION

The electric field gradient (EFG) at nuclear sites in noncubic metals is generally considered to arise from two sources. The noncubic arrangement of the positively charged lattice ions causes a lattice field gradient V_{zz}^{lat} , and the nonuniform charge density of the conduction electrons leads to an electronic contribution V_{zz}^{el} . The lattice EFG V_{zz}^{lat} is easily calculated by a lattice sum calculation, and its enhancement by the quadrupole deformation of the closed electronic shells of the probe atom can be taken into account by the Sternheimer correction factor $(1-\gamma_\infty)$. The conduction-electron contribution, however, is difficult to evaluate theoretically, since in principle the conduction-electron wave functions and the densities of states in pure metals and impurity-metal systems must be known.

Therefore systematic experimental studies of the EFG have been performed in recent years. Both the sign and magnitude of the EFG have been determined in a large number of pure metals and impurity-host combinations.¹ Furthermore the dependence of the EFG on temperature and pressure has been investigated in many cases.^{2,3}

These experimental data have revealed two rather general properties of the EFG in noncubic metals:

- (i) When analyzing those cases where the sign of

the EFG could be determined, Raghavan *et al.*⁴ found a "universal correlation" between V_{zz}^{el} and $(1-\gamma_\infty)V_{zz}^{\text{lat}}$: In a large number of cases the electronic EFG is approximately three times larger than the ionic EFG $(1-\gamma_\infty)V_{zz}^{\text{lat}}$ and has the opposite sign

$$V_{zz}^{\text{el}} = -k(1-\gamma_\infty)V_{zz}^{\text{lat}}, \quad k \approx 3. \quad (1)$$

- (ii) In most pure metals and impurity-host combinations the temperature dependence of the EFG is much stronger than expected from the lattice expansion and can be described very precisely by the simple relation²

$$V_{zz}(T)/V_{zz}(0) = 1 - BT^{3/2}, \quad (2)$$

where B is a positive constant, which depends on host and impurity properties.

Recently some progress has been made towards an understanding of these two phenomena. Bodendstedt and Perscheid⁵ have proposed a simple model to explain the "universal correlation". The strong temperature dependence of the EFG and the $T^{3/2}$ relation are now generally attributed to thermal vibrations of the probe and the lattice atoms which tend to reduce the EFG at high temperatures.⁵⁻⁷ A completely satisfactory theory of the EFG in metals, however, is still missing, and therefore further experimental information on the EFG is of interest.

In this paper we report a systematic study of the EFG at dilute ^{181}Ta impurities in the heavy-rare-earth metals Gd, Dy, Ho, and Er, which was performed with the time-differential perturbed-angular-correlation (TDPAC) technique.

The heavy-rare-earth metals Gd to Tm are very similar in their chemical and crystallographic properties. They appear all to be group-IIIa elements like yttrium. This is because the 4*f* electronic shell is being filled at this point of the Periodic Table, while the number of outer valence electrons remains unchanged. The 4*f* shell is well localized inside the electron core and has therefore little influence on the chemical bonding.

The EFG acting on the rare-earth nuclei is mainly determined by the large contribution coming from the open 4*f* shell. For impurities on substitutional lattice sites, however, the 4*f* electrons contribute—if at all—only very little to the EFG because of their strong localization inside the rare-earth ion cores, and therefore the main contributions should come from the lattice ions (V_z^{lat}) and the conduction electrons (V_z^{el}). All heavy rare-earth metals, with the exception of Yb crystallize in a hexagonal close packed lattice structure. The lattice parameters *c* and *a* change very little across the rare-earth series, and therefore also the lattice EFG changes only slightly between Gd and Tm. Previous investigations of the EFG at the impurities ^{111}Cd and ^{181}Ta in the rare-earth metals at room temperature,⁸⁻¹⁰ however, revealed a rather strong variation of the effective EFG across the rare-earth series, which must be attributed to a pronounced change of the conduction electron EFG between Gd and Tm. The present investigation of the temperature dependence of the EFG at ^{181}Ta in the heavy rare-earth metals was carried out with the aim to gain more insight into the properties of the conduction-electron EFG in these metals.

II. EXPERIMENTAL DETAILS

The 133–482-keV $\gamma\gamma$ cascade of ^{181}Ta , which is populated by the β decay of the 45-day-isotope ^{181}Hf is particularly well suited for the application of the TDPAC technique because of its strong intensity, the large anisotropy $A_2 \approx -0.27$, and the half-life of the intermediate state at 482 keV of 10.8 nsec.

For the sample preparation the rare-earth metals (purity 99.9%) were alloyed with small amounts of radioactive Hf metal in a vacuum of 10^{-6} Torr by means of an electron gun. Temperatures of more than 3000 K can be reached. During the melting process the metals were placed on a water-cooled copper block. Therefore the samples cool down rapidly to room temperature as soon as the electron beam is turned off. This is important in order to avoid a possible trapping of mobile oxygen and nitrogen at the Hf impurities. The Hf concentration of

the samples was in most cases 2000 ppm. Some of the samples were annealed at 1200 K for several days and then rapidly cooled down to room temperature. Most of the measurements, however, were performed with unannealed sources.

The time-differential perturbed angular correlation was measured with a four-detector apparatus, which is described in detail in Ref. 11. The electronic set-up consists of four independent fast-slow coincidence circuits, including time-to-amplitude converters and permits simultaneously four independent measurements of the same angular correlation.

The time spectra of the coincidences $N(\theta, t)$ of the 133–482-keV cascade of ^{181}Ta were taken at the angles $\theta = 90, 135, \text{ and } 180^\circ$ and were stored for each coincidence circuit into a 256 channel subgroup of a 4096 channel analyzer. The four time spectra recorded at each angle were corrected for accidental coincidences and small source misalignments and were added after normalization of the time calibrations and the time zero points. From these added time spectra the perturbation factors $A_2 G_{22}(t)$ were calculated, using the relation

$$N(\theta, t) = N_0 e^{-t/\tau} [1 + A_2 G_{22}(t) P_2(\cos\theta) + A_4 G_{44}(t) P_4(\cos\theta)] . \quad (3)$$

Here $P_k(\cos\theta)$ are the Legendre polynomials and τ is the lifetime of the intermediate state of the $\gamma\gamma$ cascade. A_2 and A_4 are the unperturbed angular correlation coefficients.

Measurements were carried out between the Néel temperatures, where the rare-earth metals begin to exhibit a spontaneous magnetic order, and about 600 K. Temperatures below room temperature were obtained with a liquid nitrogen cryostat, which is equipped with a small electrical heater for temperature variation. For temperatures above 290 K an electrically heated furnace was used. The temperature stability of all measurements was better than 1 degree.

In Fig. 1 a typical result obtained with an unannealed sample of Er ^{181}Ta at three different temperatures is shown. Similar spectra were obtained for Dy ^{181}Ta and Ho ^{181}Ta . The perturbation factor for Gd ^{181}Ta at 339 and 484 K is shown in Fig. 2. These latter spectra were obtained after annealing the samples at 700 K for several days and subsequent rapid quenching to room temperature. The Hf concentration of these samples was 200 ppm. Without annealing and quenching only a strongly damped spectrum without any oscillation was observed. When the sample was heated above 500 K, the oscillation disappeared and could not be observed again upon cooling to lower temperatures. The same phenomenon has been observed by Lindgren *et al.*¹² for Tb ^{181}Ta , where the oscillation disappeared at 900 K. Lindgren *et al.*¹² suggest that at these temperatures mobile im-

purities such as oxygen and nitrogen are trapped by the Hf atoms, which would cause a broad distribution of interaction frequencies and consequently a damping of the angular correlation pattern.¹³ Another possible explanation would be that the equilibrium solu-

bility of Hf in Gd and Tb is extremely small and that by quenching metastable solid solutions of Hf in Gd and Tb are formed which decompose at higher temperatures.

The equilibrium solubility of Hf in the rare-earth metals has not been investigated in detail up to now. To our knowledge the equilibrium phase diagram has been determined only for the system Hf-Er,¹⁴ in which the Hf solubility at room temperature is 3 at.%. An estimate of the Hf solubility in the other rare-earth metals may be obtained by comparison with the Zr-R-systems.¹⁵ These data suggest that the equilibrium solubility of Hf in the rare-earth metals decreases very strongly between Er and Gd, and it cannot be excluded that at equilibrium conditions Hf is not soluble at all in Gd and Tb. On the other hand, Wang *et al.*¹⁶ have shown that rapid quenching of Hf-R alloys leads to metastable systems with an increased Hf solubility. It is therefore conceivable that the irreversible changes of the TDPAC spectra of Gd¹⁸¹Ta at 500 K and Tb¹⁸¹Ta at 900 K are due to the decomposition of a metastable phase formed by quenching of the samples.

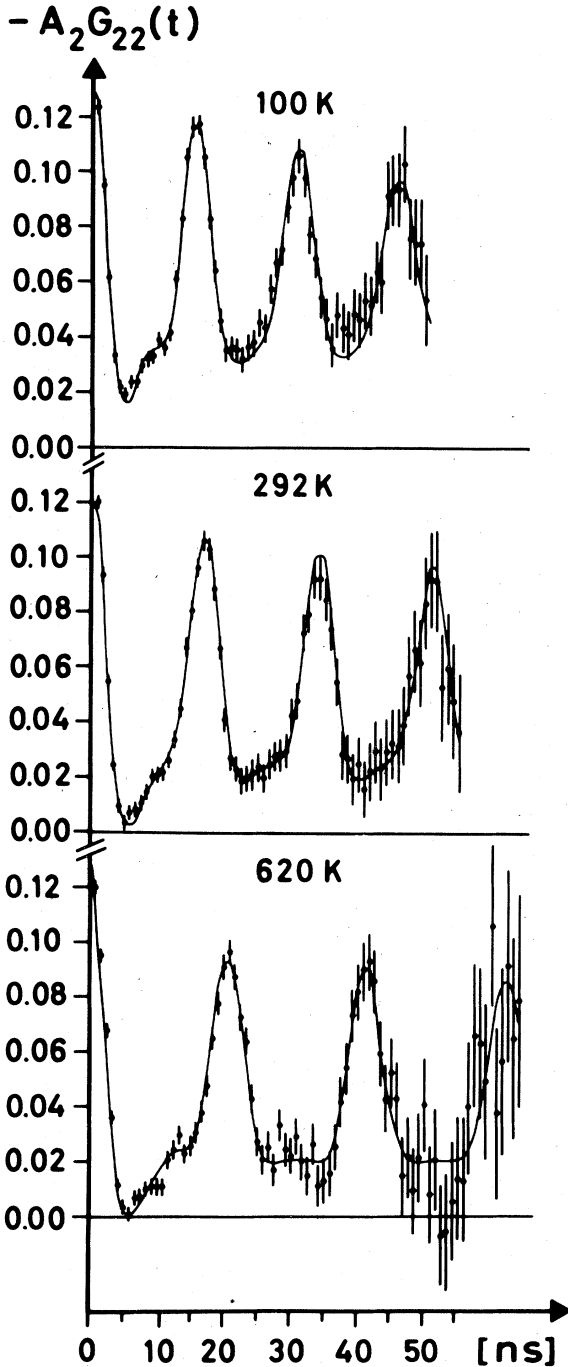


FIG. 1. TDPAC spectra of Er¹⁸¹Ta at different temperatures.

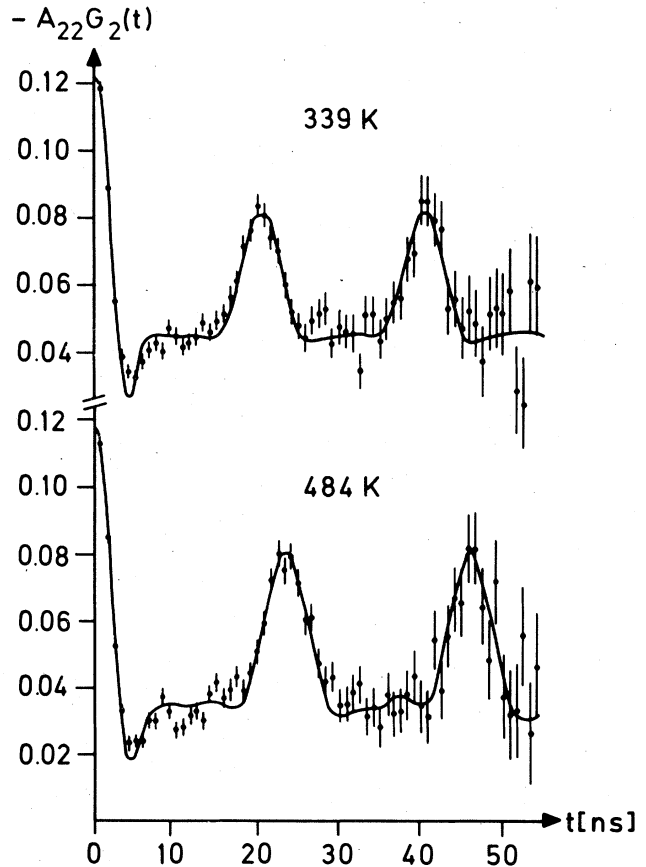


FIG. 2. TDPAC spectra of Gd¹⁸¹Ta at 339 and 484 K.

III. DATA TREATMENT AND RESULTS

The theoretical perturbation factor for an electric quadrupole interaction in a polycrystalline sample is given by the expression,¹⁷

$$G_{kk}(t) = \sigma_{k0} + \sum_{n=1}^N \sigma_{kn} \cos(\omega_n t) \exp\left(-\frac{1}{2} \omega_n^2 \delta^2 t^2\right). \quad (4)$$

The number N of terms in this formula depends on the nuclear spin I of the intermediate state of the $\gamma\gamma$ cascade. For the present case of ^{181}Ta with $I = \frac{5}{2}$ one has $N = 3$. The frequencies ω_n in Eq. (4) correspond to the transition frequencies between the hyperfine sublevels into which the intermediate state of the cascade is split by the hyperfine interaction. The frequencies ω_n and the amplitudes σ_{kn} are functions of the quadrupole frequency ν_Q and the asymmetry parameter η , defined as,¹⁸

$$\nu_Q = \frac{eQV_{zz}}{h}, \quad \eta = \frac{V_{yy} - V_{xx}}{V_{zz}}. \quad (5)$$

V_{xx} , V_{yy} , and V_{zz} are the components of the EFG tensor and Q is the nuclear quadrupole moment. The exponential factor in Eq. (4) has been included to allow for a possible Gaussian distribution of the EFG values, which manifests itself by a damping of the oscillation amplitudes. The relative width of this distribution is described by the parameter δ .

For impurities on a substitutional site of a hexagonal lattice one expects an axially symmetric EFG ($\eta = 0$). The corresponding perturbation factor is a periodic, undamped function of time. The measured spectra $A_2 G_{22}(t)$ (see Figs. 1 and 2) show almost undamped oscillations at large delay times. The anisotropy at $t = 0$, however is considerably larger than the amplitude of these undamped oscillations. Furthermore, in the first minimum the anisotropy is smaller than in the other minima. This behavior suggests that a fraction f of the impurities occupies regular substitutional sites, where they are subject to a nearly unique electric hyperfine interaction, while the rest $(1-f)$ of the impurities experiences a broad distribution of different EFG values. Therefore the expression

$$A_2 G_{22}(t) = A_{22} [f G_{22}^{\text{reg}}(t) + (1-f) G_{22}^{\text{irr}}(t)] \quad (6)$$

was fitted to the measured spectra. $G_{22}^{\text{reg}}(t)$ is the perturbation factor [Eq. (4)] for the regular site fraction, for which we admitted a small Gaussian frequency distribution of relative width δ . $G_{22}^{\text{irr}}(t)$ is the perturbation factor for those nuclei which are subject to a broad frequency distribution of relative width δ' . In the least-squares fitting routine the fraction f , ν_Q , η , and δ for the regular site fraction, and ν_Q' , η' , and δ' for the irregular site fraction were treated as free parameters. The coefficients σ_{kn} and σ_{kn}' were not allowed to vary independently, but treated as

functions of the quadrupole frequency and the asymmetry parameter.¹⁸ The finite time resolution of the coincidence circuits was taken into account by folding Eq. (6) with the time response curve.

The quantities of main interest are the quadrupole frequency ν_Q and the fraction f of impurities on regular lattice sites with an unperturbed environment. The results for these two quantities are listed in Table I for the different rare-earth hosts and temperatures. The asymmetry parameter of the regular site fraction was in all cases $\eta \leq 0.05$, and the relative width of the frequency distribution $\delta \leq 0.03$. For the irregular site fraction the fits yielded a broad frequency distribution with a center frequency $\nu_Q' \approx 400$ MHz, and a relative width $\delta' \approx 0.30$.

The values in Table I show that in the case of Dy, Ho, and Er 50–60% of the Hf atoms occupy regular lattice positions, while for Gd f is only 0.2. For Hf in Tb Lindgren *et al.*¹² observed a regular site fraction of $f = 0.4$. The decrease of the fraction f from the group Er, Ho, Dy to Tb and Gd possibly is a further indication for a decrease of the equilibrium solubility of Hf in the rare-earth metals. The Hf solubility, however, cannot be the only factor which determines the magnitude of f . For Hf in Er one would expect $f = 1$, since the Hf solubility is 3 at.% and our samples had a Hf concentration of 0.2 at.%. The experimental value $f = 0.6$ shows that a large number of Hf atoms, even if they are on substitutional sites, must have a perturbed environment, possibly due to the trapping of other impurities such as oxygen and nitrogen.

IV. DISCUSSION

From the measured quadrupole frequency ν_Q we have calculated the electric field gradient V_{zz} using $Q = 2.51$ barn¹⁹ for the electric quadrupole moment of the 482-keV state of ^{181}Ta . The values of V_{zz} are listed in the fourth column of Table I. The previously reported⁹ room-temperature value of V_{zz} for Er ^{181}Ta is incorrect, probably due to a defect of the multichannel analyzer. Column five of Table I contains the values of the lattice EFG V_{zz}^{lat} . These values were calculated from the lattice parameters c and a by means of the expression

$$V_{zz}^{\text{lat}} = \frac{Ze}{4\pi\epsilon_0} \left[0.0065 - 4.3584 \left(\frac{c}{a} - 1.6333 \right) \right] / a^3, \quad (7)$$

which has been derived by Das and Pommerantz²⁰ for a point charge hexagonal lattice. Z is the valence of the lattice ions. For the rare-earth metals we assumed $Z = +3$. The lattice parameters c and a of the rare-earth metals have been measured by Finkel *et al.*^{21–24} for temperatures below 290 K, and the Spedding *et al.*²⁵ for temperatures above 290 K. At $T = 290$ K the values of c and a given by Spedding

TABLE I. The quadrupole frequency ν_Q , the regular site fraction f , the electric field gradient V_{zz} , the lattice field gradient V_{zz}^{lat} , and the ratio $\alpha = |V_{zz}/(1 - \gamma_\infty)V_{zz}^{\text{lat}}|$ for ^{181}Ta in the heavy-rare-earth metals Gd, Dy, Ho, and Er at different temperatures. The error quoted for V_{zz} does not contain the uncertainty of the nuclear quadrupole moment.

	T (K)	ν_Q (MHz)	f	V_{zz} (10^{17}V/cm^2)	V_{zz}^{lat} (10^{15}V/cm^2)	$\alpha = \frac{V_{zz}}{(1 - \gamma_\infty)V_{zz}^{\text{lat}}}$
Gd	339	324.2(8.7)	0.21(3)	5.34(14)	1.79	4.82(13)
	484	282.3(9.9)	0.13(2)	4.65(16)	1.76	4.27(15)
Dy	192	414.9(10.0)	0.56(5)	6.83(17)	2.53	4.37(11)
	240	398.6(8.1)	0.67(5)	6.57(13)	2.49	4.26(8)
	290	394.7(9.4)	0.59(5)	6.50(16)	2.48	4.22(10)
	457	350.2(9.8)	0.69(5)	5.77(16)	2.37	3.92(11)
	589	317.9(7.9)	0.69(5)	5.24(13)	2.26	3.74(10)
Ho	151	424.5(9.2)	0.51(5)	6.99(16)	2.77	4.05(10)
	233	407.3(8.7)	0.55(5)	6.71(14)	2.73	3.97(10)
	290	396.3(7.0)	0.49(5)	6.53(12)	2.68	3.92(8)
	373	372.0(9.1)	0.45(5)	6.12(16)	2.60	3.79(10)
	473	349.1(7.6)	0.51(5)	5.75(13)	2.52	3.68(8)
Er	595	320.7(7.2)	0.48(5)	5.29(13)	2.41	3.55(8)
	100	430.4(9.0)	0.52(5)	7.09(16)	2.87	3.98(10)
	150	423.6(8.9)	0.54(5)	6.98(16)	2.82	3.98(10)
	200	411.6(9.4)	0.51(5)	6.78(16)	2.78	3.94(10)
	290	387.3(7.1)	0.62(5)	6.38(13)	2.68	3.84(8)
	387	369.0(7.5)	0.53(5)	6.08(13)	2.58	3.81(10)
	495	344.2(7.1)	0.53(5)	5.67(13)	2.48	3.69(10)
	620	315.8(7.0)	0.52(5)	5.20(13)	2.37	3.53(10)

*et al.*²⁵ differ by 10^{-3} from those measured by Finkel *et al.*²¹⁻²⁴ This difference in the lattice parameters causes a difference in V_{zz}^{lat} of about 3%. To avoid a discontinuity in the temperature dependence of V_{zz}^{lat} , we have normalized the high-temperature values of V_{zz}^{lat} to Finkel's value of 290 K.

The point-charge lattice EFG given by Eq. (7) is enhanced by the quadrupole moments induced in the rare-earth ion cores and the quadrupole moments of the open $4f$ electronic shell. Estimates based on the formulas given by Das and Ray,²⁶ however, show that these contributions of V_{zz}^{lat} are negligibly small.

A. Room-temperature results

The room-temperature values of the measured EFG for ^{181}Ta and the calculated lattice EFG V_{zz}^{lat} are displayed in Fig. 3 as a function of the rare-earth metal hosts. In addition Fig. 3 shows the variation of EFG at the impurity ^{111}Cd between Gd and Er.⁸ For both impurities V_{zz} first increases, reaches a maximum in the middle of the series, and then decreases again, whereas V_{zz}^{lat} increases continuously between Gd and Er by roughly 15%. This difference in the behavior of V_{zz} and V_{zz}^{lat} is illustrated in a different

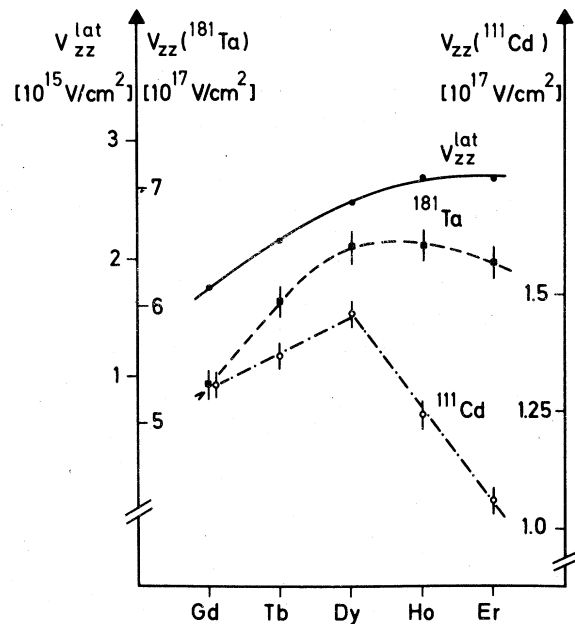


FIG. 3. Measured electric field gradient V_{zz} at the impurities ^{181}Ta and ^{111}Cd and the calculated lattice field gradient V_{zz}^{lat} at room temperature as a function of the rare-earth atomic number.

way in Fig. 4. Here we have plotted the ratio

$$\alpha = \left| \frac{V_{zz}}{(1 - \gamma_{\infty}) V_{zz}^{\text{lat}}} \right|, \quad (8)$$

for ^{111}Cd and ^{181}Ta as a function of the rare-earth atomic number. For the calculation of α the free ion Sternheimer corrections $(1 - \gamma_{\infty}) = 62$ for Ta^{5+} and $(1 - \gamma_{\infty}) = 31$ for Cd^{2+} (Ref. 27) were used. For both impurities the enhancement factor α decreases between Gd and Er, for ^{111}Cd by roughly 50% and for ^{181}Ta by 20%. To a good approximation the decrease is a linear function of the rare-earth atomic number N with $N(\text{Gd}) = 0$,

$$\alpha(R) = \alpha(\text{Gd})(1 - \epsilon N). \quad (9)$$

A fit of Eq. (9) to the data shown in Fig. 4 yields

$$\alpha(\text{Gd } ^{181}\text{Ta}) = 4.76(8),$$

$$\epsilon(R \text{ } ^{181}\text{Ta}) = 0.052(6),$$

$$\alpha(\text{Gd } ^{111}\text{Cd}) = 2.44(5),$$

$$\epsilon(R \text{ } ^{111}\text{Cd}) = 0.118(7).$$

The factor α is related to the electronic enhancement factor k in the "universal correlation" [Eq. (1)] proposed by Raghavan *et al.*⁴ With

$$V_{zz} = (1 - \gamma_{\infty}) V_{zz}^{\text{lat}} + V_{zz}^{\text{el}} \quad (10)$$

and Eq. (1) for V_{zz}^{el} one obtains

$$V_{zz} = (1 - k)(1 - \gamma_{\infty}) V_{zz}^{\text{lat}}, \quad (11)$$

so that

$$\alpha = |1 - k|. \quad (12)$$

The fitted values of $\alpha(\text{Gd} : I)$ and $\epsilon(R : I)$ ($I = ^{181}\text{Ta}, ^{111}\text{Cd}$) show that the factor k is not a constant for all impurity-host combinations, but depends on host and impurity properties.

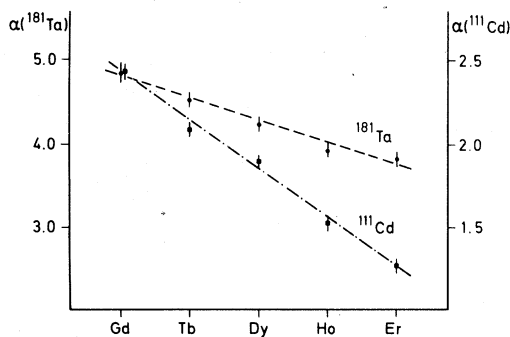


FIG. 4. Ratio $\alpha = |V_{zz}/(1 - \gamma_{\infty}) V_{zz}^{\text{lat}}|$ for the impurities ^{181}Ta and ^{111}Cd at room temperature as a function of the rare-earth atomic number.

The linear decrease of α across the rare-earth series and the different values and slopes of α for the two impurities can be understood, if one assumes (i) that the conduction-electron EFG V_{zz}^{el} is mainly determined by the number of electrons in the Wigner-Seitz cell of the impurity and (ii) that the electron density at the site of a given impurity in the rare-earth metals decreases from Gd to Er. Experimental support for the first assumption comes from the work of Soares *et al.*²⁸ and Bodenstedt *et al.*,⁵ who point out that a linear dependence of the enhancement factor k on the chemical valence Z' of various impurities in Zn exists. This suggests that the main contributions to the electron cloud surrounding the impurity come from the impurity itself and the 12 nearest rare-earth neighbors. The impurity contributes Z' electrons and each of the nearest-neighbors $\frac{1}{12}Z$ electrons. Therefore $Z + Z'$ may perhaps be taken as a measure of the conduction-electron charge in the Wigner-Seitz cell of the impurity.²⁹

For a given impurity with valence Z' the electron density most probably decreases between Gd and Er: The increase of the nuclear charge across the rare-earth series is only partially shielded by the increasing number of $4f$ electrons. As a consequence the attractive potential of the rare-earth ions increases and the conduction electrons will be concentrated nearer to the rare-earth sites. In pure rare-earth metals this effect leads to the well-known lanthanide contraction. At impurity sites this effect will result in a decrease of the total conduction-electron charge.

With these two assumptions we may then write in extension of the Raghavan correlation

$$V_{zz}^{\text{el}} = -[Z + Z' - (\Delta Z)N]k'(1 - \gamma_{\infty})q_{zz}^{\text{lat}}, \quad (13)$$

where ΔZ is the decrease of the conduction-electron charge at the impurity site between two rare-earth hosts. N is the relative rare-earth atomic number with $N(\text{Gd}) = 0$. It is assumed that the conduction-electron distribution has the same symmetry as the host lattice. Therefore V_{zz}^{el} is proportional to $q_{zz}^{\text{lat}} \equiv V_{zz}^{\text{lat}}/Z$ [Eq. (7)]. k' is a different constant than k .

With Eqs. (10), (12), and (13) this model yields for the enhancement factor α

$$\alpha(R) = \alpha(\text{Gd}) \left(1 - \frac{k'Z}{k'(Z + Z') - Z} \frac{\Delta Z}{Z} N \right) \quad (14)$$

and

$$\alpha(\text{Gd}) = \left| 1 - k' \frac{Z' + Z}{Z} \right|. \quad (15)$$

The host dependence of α is determined by $\Delta Z/Z$, the impurity dependence—apart from $1 - \gamma_{\infty}$ —by the impurity valence Z' . The constant k' and $\Delta Z/Z$ should be independent of the impurity.

$\Delta Z/Z$ and k' can be calculated from the measured

values of $\alpha(\text{Gd})$ and $\epsilon(R)$ for the two impurities. With $Z' = +2$ for Cd, $Z' = +5$ for Ta, and $Z = +3$ for the rare-earth metals one obtains

$$k' = 2.11(3), \quad \Delta Z/Z = 0.12(1), \quad \text{for Ta,}$$

$$k' = 2.16(3), \quad \Delta Z/Z = 0.14(1), \quad \text{for Cd.}$$

Within the errors k' and $\Delta Z/Z$ have the same values for both impurities, though $\alpha(\text{Gd})$ and $\epsilon(R)$ differ by nearly a factor of 2 between Ta and Cd. It follows that Eq. (13) is a consistent parametrization of the electric field gradient for both impurities in the heavy rare-earth metals, which suggests that V_{zz}^{el} is proportional to the number of electrons surrounding the impurity and that its impurity dependence in a given host can be approximated by the factor $(1 - \gamma_{\infty})(Z + Z')/Z$.

The deduced average charge decrease $\Delta Z/Z = 0.13$ does not appear to be unrealistic. A charge decrease at the impurity site is equivalent to a displacement of the conduction-electron charge distribution. If one assumes that this charge distribution is centered in the middle between the impurity and the nearest rare-earth neighbor, then one may estimate from the $1/r^3$ dependence of the EFG that $\Delta Z/Z = 0.13$ corresponds to a displacement of 2.5% of the lattice parameters. As shown by Hartree-Fock calculations, the lanthanide contraction of the free rare-earth atoms, i.e., the decrease of the radius of the maximum charge density of the 6s electrons is of the same order of magnitude.³⁰

B. Temperature dependence of the EFG

In Fig. 5 the quadrupole frequency ν_Q of ^{181}Ta and the calculated lattice EFG (solid lines) are shown as a function of temperature for the different rare-earth hosts. A linear temperature scale has been used. One notes two interesting aspects: In all cases the quadrupole frequency is to a very good approximation a linear function of temperature, in contrast to the $T^{3/2}$ relation [Eq. (2)] observed in many other systems. The quadrupole frequency decreases stronger with temperature than the calculated lattice EFG. However, the difference in the slopes of ν_Q and V_{zz}^{lat} is much larger for Gd than for Er.

To parametrize the linear temperature dependence of ν_Q , we have fitted the expression

$$\nu_Q(T) = \nu_Q(0)(1 - AT) \quad (16)$$

to the experimental data. The results obtained for $\nu_Q(0)$ and A are listed in Table II. The large errors of $\nu_Q(0)$ and A for Gd are due to the fact that in this host ν_Q could be measured at two temperatures only. The data for Tb have been taken from Ref. 12.

The extrapolated quadrupole frequency $\nu_Q(0)$ varies roughly in the same way with the rare-earth atomic number as ν_Q measured at room temperature.

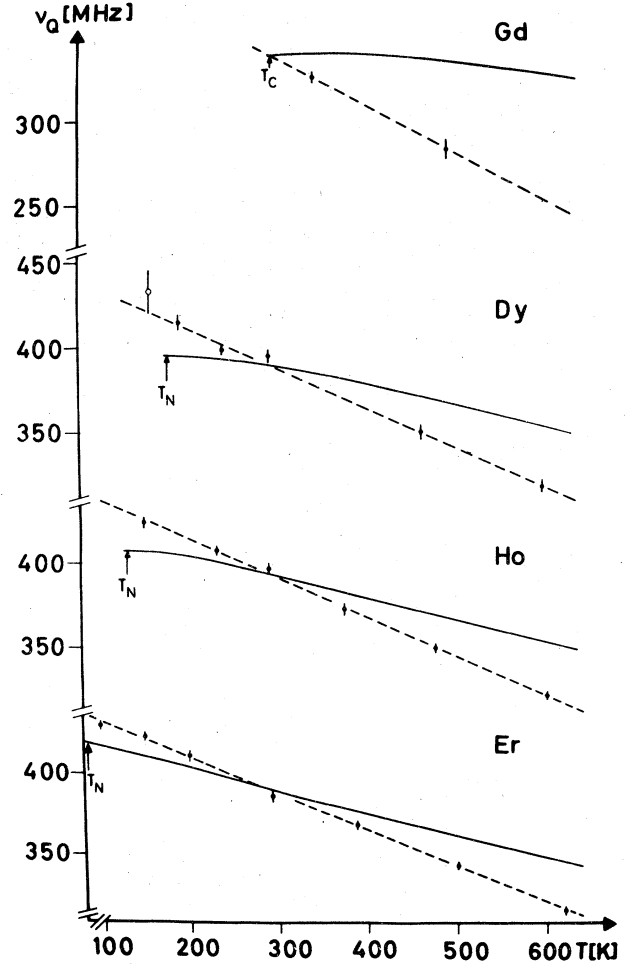


FIG. 5. Temperature dependence of the electric quadrupole frequency ν_Q of ^{181}Ta in the rare-earth metals Gd, Dy, Ho, and Er. The dotted lines represent fits of Eq. (16) to the data. The solid lines show the temperature dependence of the lattice field gradient V_{zz}^{lat} .

TABLE II. The parameters $\nu_Q(0)$ and A for the different rare-earth hosts, obtained by fitting Eq. (16) to the experimental values of ν_Q .

Host	$\nu_Q(0)$ (MHz)	A (K^{-1})
Gd	422.1(12.0)	$6.8(1.5) \times 10^{-4}$
Tb	457.5(5.0)	$7.2(4) \times 10^{-4}$
Dy	460.7(4.1)	$5.22(15) \times 10^{-4}$
Ho	462.2(1.8)	$5.14(10) \times 10^{-4}$
Er	454.9(1.5)	$4.92(7) \times 10^{-4}$

The relative temperature dependence, expressed by the parameter A , decreases from Gd and Tb to the group Dy, Ho, Er, for which A has practically the same value. There are several impurity host systems in which the EFG does not follow a $T^{3/2}$ relation.³¹⁻³³ For Fe in Be a quadratic dependence at low temperatures goes to a linear dependence at higher temperatures.³¹ A linear temperature dependence has also been found for Yb in Tm,³² and for Rh in the intermetallic compound PdPb₂.³³ These deviations from the $T^{3/2}$ relation are in some cases attributed to an open electronic shell at the impurity. It may be possible that such effects have an influence also on the temperature dependence of the EFG of ¹⁸¹Ta in the rare-earth metals. The valence shell of the Ta atom has the configuration $5d^36s^2$ and therefore a contribution to the EFG from d electrons localized at the impurity cannot be excluded. There is some experimental information suggesting a local d -electron contribution for Ta in the rare-earth metals: The systematics of the magnetic hyperfine field at $5d$ impurities in Gd (Refs. 34 and 35) indicates the existence of a local magnetic moment at Ta in Gd, and the values of the EFG of $5d$ -impurities in Gd (Refs. 34 and 35) show that the electronic contribution V_{zz}^{el} depends sensitively on the number of $5d$ electrons of the impurity.

Rasera *et al.*³⁶ who have investigated the temperature dependence of the EFG of ¹⁸¹Ta in Ho, suggest that the deviation from the $T^{3/2}$ relation is related to the aspherical $4f$ charge distribution of the rare-earth host ions, which is mediated to the impurity site by the conduction electrons. The asphericity of the $4f$ charge distribution depends on the occupation of the $4f$ crystal-field states and is therefore temperature dependent. This could affect the temperature dependence of the EFG. Rasera *et al.*³⁶ therefore propose the following extension of Eq. (2):

$$V_{zz}(T) = V_{zz}(0)(1 - BT^{3/2}) \times [1 - C \langle 3J_z^2 - J(J+1) \rangle_T] . \quad (17)$$

J is the angular momentum of the ground state of the rare-earth ions, $\langle 3J_z^2 - J(J+1) \rangle_T$ describes the asphericity of the $4f$ charge distribution, i.e., the quadrupole moment of the rare-earth ions and is calculated by quantum mechanical and thermal averaging over all crystal-field states. The constant C in this model is a measure of the conduction-electron coupling between the rare-earth ions and the impurity. We have fitted Eq. (17) to our data for Dy, Ho, and Er. In the cases of Gd and Tb the number of data points is too small to allow a fit. The average $\langle 3J_z^2 - J(J+1) \rangle_T$ was calculated using the crystal-field parameters of the pure rare-earth metals measured by Touborg.³⁷ The values of the free param-

TABLE III. The parameters $V_{zz}(0)$, B , and C for ¹⁸¹Ta in Dy, Ho, and Er, obtained by fitting Eq. (17) to the experimental values of V_{zz} .

Host	$V_{zz}(0)$ (10^{17} V/cm ²)	B (10^{-5} K ^{-3/2})	$10^3 C$
Dy	6.79(31)	1.69(20)	6.2(6.2)
Ho	6.91(19)	1.71(14)	11.7(8.2)
Er	6.85(11)	1.63(10)	-7.6(2.7)

eters $V_{zz}(0)$, B , and C obtained from the fit are listed in Table III. In all cases the temperature dependence of the EFG is well described with these parameters, which agree within the errors with the values obtained by Rasera *et al.* for Ho (Ref. 36) and Er.³⁸

Within the errors the parameters $V_{zz}(0)$, B , and C have the same absolute value for the three rare-earth hosts. This does not necessarily imply that the aspherical $4f$ charge distribution really influences the EFG at impurity sites to a large extent. Rasera *et al.*³⁶ argue that their model is strongly supported by the temperature dependence of the EFG of ¹⁸¹Ta in Lu, which has been measured by Butz *et al.*³⁹ Lu has a completely filled $4f$ shell and the charge distribution of the Lu ions is spherically symmetric, i.e., the term $\langle 3J_z^2 - J(J+1) \rangle_T$ in Eq. (17) vanishes. Therefore the EFG should follow a $T^{3/2}$ relation, in contrast to rare-earth hosts with incomplete $4f$ shells. Rasera *et al.*³⁶ assume this to be true. In our opinion, however the data of Butz *et al.*³⁹ for Lu ¹⁸¹Ta between 4.2 and 450 K can equally well—perhaps even better—be described by a linear function of temperature, as for the other rare-earth metals with incomplete $4f$ shells. Further accurate data with other impurities appear necessary for a final conclusion.

In order to compare the temperature dependence of the measured EFG to that of the calculated lattice EFG, we have determined the ratio

$$\alpha = |V_{zz}/(1 - \gamma_\infty) V_{zz}^{lat}|$$

for the different temperatures. The values of α listed in column six of Table I show that α decreases with increasing temperature. Within the errors this decrease can be described by a linear function of temperature

$$\alpha(T) = \alpha(0)(1 - \beta T) . \quad (18)$$

In Fig. 6 the slope $\beta = -d[\alpha/\alpha(0)]/dT$, as obtained from fits of Eq. (18) to the values of $\alpha(T)$, is displayed as a function of the rare-earth atomic number. The values for TbTa and LuTa have been calculated from the data in Refs. 12 and 39. It is a

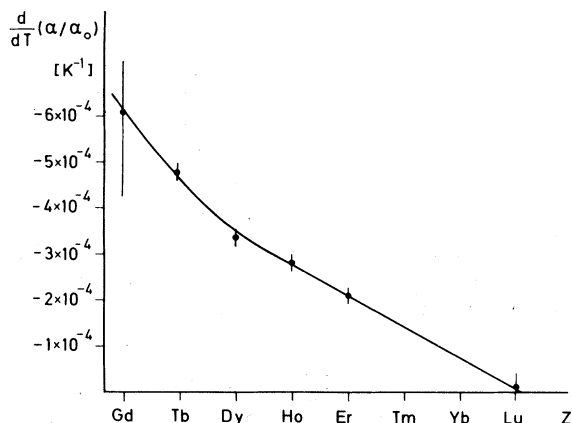


FIG. 6. Slope $d[\alpha/\alpha(0)]/dT$ as a function of the rare-earth atomic number.

remarkable result that $d[\alpha/\alpha(0)]/dT$ decreases continuously from Gd to Lu, where V_{zz} and V_{zz}^{lat} have the same temperature dependence.

The larger the value of $d[\alpha/\alpha(0)]/dT$, the more

the temperature dependence of V_{zz} differs from that of V_{zz}^{lat} . Lattice vibrations tend to reduce the EFG, relative to V_{zz}^{lat} calculated from the lattice parameters. The continuous decrease of $d[\alpha/\alpha(0)]/dT$ may therefore indicate a decrease of the amplitude of the lattice vibrations across the rare-earth series. Such an explanation is supported by the increase of the Debye temperature and the melting point between Gd and Lu. A more detailed analysis is not possible as long as no experimental information on the phonon spectra of the rare-earth metals is available.

ACKNOWLEDGMENTS

The authors are indebted to Professor E. Bodenstedt for his kind interest and support of this work. The numerical calculations were performed on the IBM 370/168 computer of the Regionales Hochschulrechenzentrum der Universität Bonn. The generous financial support by the Bundesminister für Forschung und Technologie is gratefully acknowledged.

- ¹R. Vianden, *Hyperfine Interact.* **4**, 956 (1978).
- ²J. Christiansen, P. Heubes, R. Keitel, W. Klinger, W. Loeffler, W. Sandner, and W. Witthuhn, *Z. Phys. B* **24**, 177 (1976).
- ³T. Butz, *Phys. Scr.* **17**, 87 (1978); **17**, 445 (1978).
- ⁴R. S. Raghavan, E. N. Kaufmann, and P. Raghavan, *Phys. Rev. Lett.* **34**, 1280 (1975).
- ⁵E. Bodenstedt and B. Perscheid, *Hyperfine Interact.* **5**, 291 (1978).
- ⁶K. Nishiyama, F. Dimmling, T. Kornrumpf, and D. Riegler, *Phys. Rev. Lett.* **37**, 357 (1976).
- ⁷P. Jena, *Phys. Rev. Lett.* **36**, 418 (1976).
- ⁸J. B. Fechner, M. Forker, and B. Schäfer, *Z. Phys.* **265**, 179 (1973).
- ⁹M. Forker, J. B. Fechner, and H. Haverkamp, *Z. Phys.* **269**, 279 (1974).
- ¹⁰M. Forker and A. Hammesfahr, *Z. Phys.* **260**, 131 (1973).
- ¹¹H. F. Wagner and M. Forker, *Nucl. Instrum. Methods* **69**, 197 (1969).
- ¹²B. Lindgren and T. Butz, Uppsala University Report UIIP-972 (1978) (unpublished).
- ¹³M. Forker, *Nucl. Instrum. Methods* **106**, 121 (1973).
- ¹⁴E. M. Savitsky, V. F. Terekhova, R. S. Torchinova, I. A. Markova, O. P. Naumkin, V. E. Kolesnichenko, and V. F. Strononova, in *Les elements des Terres Rares Paris-Grenoble, 1969*, Colloq. Int. Cent. Nat. Rech. Sci. No. 180 (CNRS, Paris, 1970).
- ¹⁵G. W. Cunningham, *Reactor Core Mater.* **3**, 28 (1960).
- ¹⁶R. Wang and Y. B. Kim, *Met. Trans.* **5**, 1973 (1974).
- ¹⁷H. Frauenfelder and R. M. Steffen, in *Perturbed Angular Correlations*, edited by K. Karlsson, E. Matthias, and K. Siegbahn (North-Holland, Amsterdam, 1963).
- ¹⁸E. Gerdau, J. Wolf, H. Winkler, and J. Braunsfurth, *Proc. R. Soc. London Ser. A* **311**, 197 (1969).
- ¹⁹G. Netz and E. Bodenstedt, *Nucl. Phys. A* **208**, 503 (1973).
- ²⁰T. P. Das and M. Pommerantz, *Phys. Rev.* **123**, 2070 (1961).
- ²¹V. A. Finkel and M. I. Palatnik, *Sov. Phys. JETP* **32**, 828 (1971).
- ²²V. A. Finkel and V. V. Vorob'ev, *Sov. Phys. JETP* **24**, 524 (1967).
- ²³V. A. Finkel, Y. N. Smirnov, and V. V. Vorob'ev, *Sov. Phys. JETP* **24**, 21 (1967).
- ²⁴V. V. Vorob'ev, Y. N. Smirnov, and V. A. Finkel, *Sov. Phys. JETP* **22**, 1212 (1966).
- ²⁵F. H. Spedding, J. J. Hanak, and A. H. Daane, *J. Less Common Met.* **3**, 110 (1961).
- ²⁶K. C. Das and K. D. Ray, *Phys. Rev.* **187**, 777 (1969).
- ²⁷F. D. Feiock and W. R. Johnson, *Phys. Rev.* **187**, 39 (1969).
- ²⁸J. C. Soares, K. Krien, P. Herzog, H. R. Folle, K. Freitag, F. Reuschenbach, M. Reuschenbach, and R. Trzcinski, *Z. Phys. B* **31**, 395 (1978).
- ²⁹K. Krien (unpublished).
- ³⁰S. Fraga, J. Karwowski, and K. M. S. Saxena, *Handbook of Atomic Data* (Elsevier Scientific, Amsterdam, 1976).
- ³¹C. Janot, P. Delacroix, and M. Piecuch, *Phys. Rev. B* **10**, 2661 (1974).
- ³²A. R. Chuhuran-Long, A. Li-Scholz, and R. L. Rasera, *Phys. Rev. B* **8**, 1791 (1973).
- ³³R. Vianden and E. N. Kaufmann, *Z. Phys.* (to be published).
- ³⁴B. Perscheid, H. Büchsler, and M. Forker, *Phys. Rev. B* **14**, 4803 (1976).
- ³⁵K. Krien, M. Forker, F. Reuschenbach, and R. Trzcinski, *Hyperfine Interact.* **7**, 19 (1979).
- ³⁶R. L. Rasera, B. D. Dunlap, and G. K. Shenoy, *Phys. Rev. Lett.* **41**, 1188 (1978).
- ³⁷P. Touborg, *Phys. Rev. B* **16**, 1201 (1977).
- ³⁸R. L. Rasera (private communication).
- ³⁹T. Butz and G. M. Kalvius, *J. Phys. F* **4**, 2331 (1974).